DEVELOPMENT OF HIGH-VOLTAGE NEGATIVE ION BASED NEUTRAL BEAM INJECTOR FOR FUSION DEVICES

O. Sotnikov
BINP SB RAS
Novosibirsk, Russian Federation
Email: O.Z.Sotnikov@inp.nsk.su

A. Ivanov
BINP SB RAS
Novosibirsk, Russian Federation
Email: A.A.Ivanov@inp.nsk.su

Yu. Belchenko
BINP SB RAS
Novosibirsk, Russian Federation
Email: Yu.I.Belchenko@inp.nsk.su

A. Gorbovsky
BINP SB RAS
Novosibirsk, Russian Federation
Email: A.I.Gorbovsky@inp.nsk.su

P. Deichuli
BINP SB RAS
Novosibirsk, Russian Federation
Email: P.P.Deichuli@inp.nsk.su

A. Dranichnikov
BINP SB RAS
Novosibirsk, Russian Federation
Email: A.N.Dranitchnikov@inp.nsk.su

I. Emelev
BINP SB RAS
Novosibirsk, Russian Federation
Email: I.S.Emelev@inp.nsk.su

V. Kolmogorov
BINP SB RAS
Novosibirsk, Russian Federation
Email: V.V.Kolmogorov@inp.nsk.su

A. Kondakov
BINP SB RAS
Novosibirsk, Russian Federation
Email: A.A.Kondakov@inp.nsk.su

A. Sanin
BINP SB RAS
Novosibirsk, Russian Federation
Email: A.L.Sanin@inp.nsk.su

I. Shikhovtsev
BINP SB RAS
Novosibirsk, Russian Federation
Email: I.V.Shikhovtsev@inp.nsk.su

Abstract

A prototype of powerful high-voltage neutral beam injector, based on acceleration of negative hydrogen ions and their neutralization is under development at the Budker Institute of Nuclear Physics (BINP) [1]. The design of BINP high-voltage injector includes several innovative components, important for injector operation stability and overall efficiency: 1) multi-aperture long-pulsed surface-plasma negative ion source, 2) wide-aperture low-energy beam transport section (LEBT), 4) negative ion acceleration tube, 5) high-energy transport section, 6) plasma target for negative ions neutralization, 7) recuperators for the energy of non-neutralized ions. The several test stand facilities were constructed at BINP for injector components study. The paper describes the results of experiments on the negative ion beam production, transport through LEBT, ion acceleration to the energy up to 240 keV and transport through the high voltage beam transport section (HEBT) to the distance ~ 10 m from the source. The data on the transported beam parameters, measured at the several beam line points and at the beam dump calorimeter are presented. The beam transport efficiency as a function of various ion source, LEBT and HEBT parameters was measured and is compared with the calculated values. The data on plasma neutralization target is presented as well.

1. INTRODUCTION

The high-voltage negative ion based neutral beam injector (N-NBI) is under development at the Budker Institute of Nuclear Physics SB RAS. It includes several innovative components. According to the BINP injector scheme, the accelerator is set apart from the ion source by the LEBT section, which purify the beam from the accompanying impurities before entering the acceleration tube. LEBT tank contains the beam bending magnets and vacuum pumps. The parasitic fluxes of gas, cesium, secondary particles outgoing the ion source, and the secondary particles from accelerator are intercepted in the LEBT. The primary beam of negative ions is accelerated in the source to the energy of 120 keV, and transported to the inlet of the single-aperture multi-electrode acceleration tube. The ion source and LEBT section are placed at the isolated platform at the potential up to −880 kV with respect to the ground. The accelerated negative ions are neutralized in a plasma target. The non-neutralized fractions of the beam are separated from the neutrals and directed to the ion beam energy recuperators. This paper presents the experimental results on H- beam production and acceleration on the high voltage test stand. Data on plasma neutralization target is described as well. A description of full-scale negative ion source with the beam current up to 9 A will be shown.

2. BEAM FORMATION AND ACCELERATION

2.1. Experimental test stand

The high voltage test stand consisting of ion source, LEBT tank, acceleration tube and HEBT with calorimeter is schematically shown in Fig. 1. The negative ion beam, produced by the ion source, is shifted in the LEBT by bending magnets and directed to the acceleration tube inlet. The trajectories of H^- ions in the LEBT, acceleration tube and HEBT, calculated by COMSOL, are shown in Fig. 1 as well. The 440 mm offset between the source and high-voltage accelerator axes reduces the influx of co-streaming particles to the accelerator and prevents the positive ions and neutrals back-streaming into the ion source.

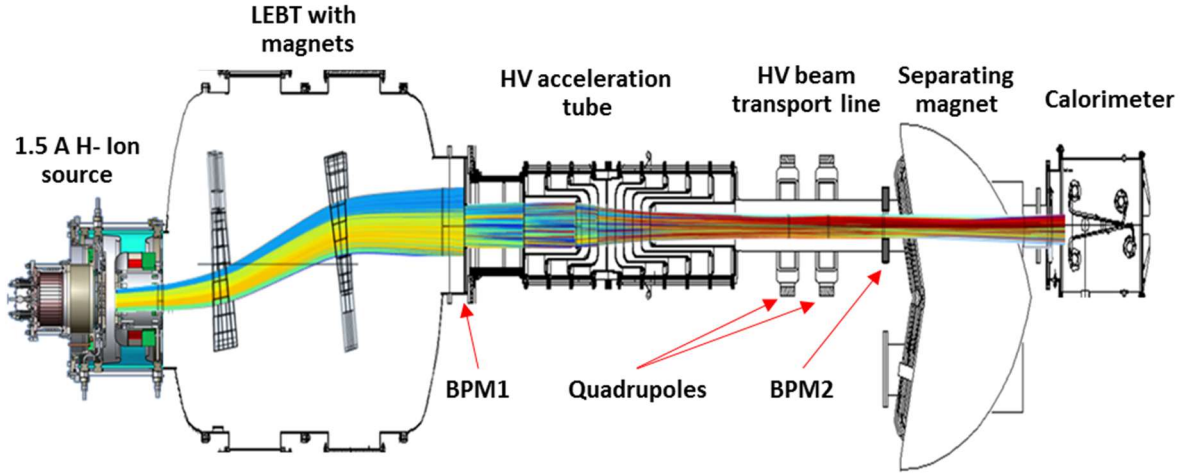

FIG. 1. Scheme of HV test stand.

The magnetic field of LEBT magnets could be varied by correction coils. It allows to control the beam turn and to match the beam with the acceleration tube. A LEBT pumping by two cryo-pumps with capacity of 100 m^3/s each provides the operational hydrogen pressure of about $\sim 10^{-3}$ Pa in the LEBT tank and in the accelerator tube during the source operation pulse. The acceleration tube consisted of 9 single aperture electrodes is projected to accelerate the beam from initial energy up to the 1 MeV. The wide aperture acceleration tube design provides an improved tube pumping and reduces the power and beam losses. The accelerated H^- beam was focused with the quadrupole lenses. The magnetic field of quadrupoles is controlled by coil currents change. The required magnetic field and coil currents are calculated by COMSOL code. The HEBT section is equipped by peripheral secondary emission detectors for beam position control (noted BPM1 and BPM2 in Fig. 1). The measurements of transported beam profile and intensity were done by water-cooled calorimeter, installed at the distance of ~ 10 m from the ion source. The separating magnet is installed before the calorimeter (Fig. 1). This magnet will be used for negative ion deflection in the future experiments.

The schematic of the acceleration tube geometry and the electric connections, used in the first experiments, are shown at the top side in Fig. 2. The single-aperture accelerating tube design increases the accelerator HV strength due to decreased secondary particles production [2]. At present, 4^{th}-8^{th} gaps were grounded, while 1^{st} – 3^{rd} gaps were successively powered up to 60 kV each. The current of accelerated beam was characterized by the total current of HV rectifier I_{HV} and by the current of the high-voltage platform I_p. The difference current I_{HV} - I_p corresponds to the sum of the intercepted currents of HV accelerator tube electrodes. During described experiments the difference current was equal to zero and $I_p = I_{HV}$, so no interception of the negative ions by the acceleration tube electrodes was registered. The trajectories in LEBT and HEBT, calculated for H^- beam, outgoing the ion source with initial divergence 30 mrad and energy 85 keV are shown in Fig. 2 (modelling by COMSOL) by the red lines. By the green lines the equipotentials are shown. As one can see, acceleration tube has 2 limiting diaphragms. The exit LEBT diaphragm with 24x24 cm^2 window was installed to cut the co-streaming flow of fast particles, created by beam stripping in vicinity of the source ion-optic system (IOS) and in the LEBT. The entrance tube electrode has the decreased aperture of ∅ 200 mm. Then the beam is accelerated in the acceleration tube. The acceleration tube provides the beam focusing by the electrostatic lens.

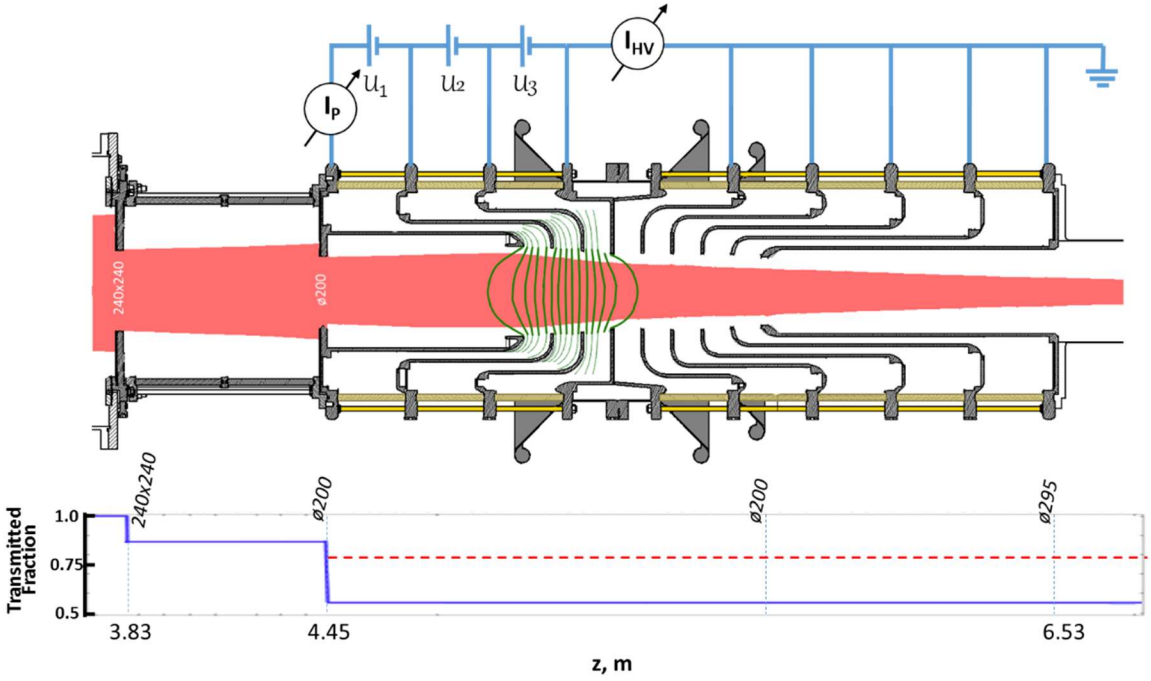

FIG. 2. At the top: the acceleration tube cross section with the scheme of electrodes powering and currents measurement. At the bottom: the fraction of H^- beam transported to the distance Z from the source (COMSOL modelling for the beam with the initial divergence 30 mrad).

Change of the beam fraction transmitted to various distance Z from the source is shown in the bottom plot in Fig. 2 (modelling by COMSOL). About 82% fraction of the 85 keV negative ion beam with initial divergence 30 mrad could be transmitted through the 240x240 mm^2 exit window of the LEBT, and about 55% beam fraction of initial beam – through the inlet tube aperture with ∅ 200 mm. It should be noted that the inlet aperture enlarging to ∅ 260 mm will increase the transmitted beam fraction to 78%, as it is shown by the red dotted line in Fig. 2).

The drawing of the BINP HV test stand is shown in Fig. 3. The H^- source with subsystems and LEBT are installed at the HV platform, negatively biased with respect to the ground. The source subsystems include RF power supply, ion beam extraction and acceleration power supplies, LAUDA thermo-stabilization system, hydrogen and cesium feeding systems. The primary power at the platform is provided via the 1 MV, 1 MW isolation transformer. As it is shown in Fig.3, each of acceleration tube gaps is powered by 110 kV voltage from the separate sections of HV rectifiers. The last electrode of accelerating tube is connected to HEBT tube and grounded.

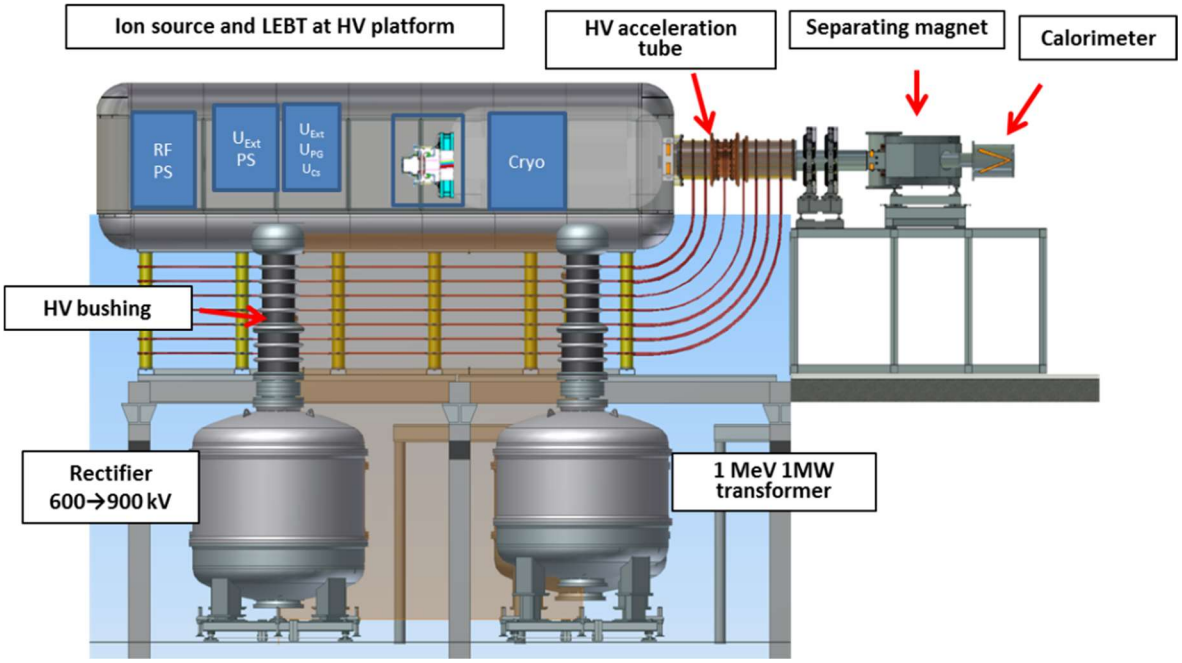

FIG. 3. 3D drawing of the BINP HV test stand.

The HV rectifiers are installed in the tanks, filled by gaseous SF_6 and equipped with the HV bushings. They are connected in series to the acceleration tube electrodes. The primary power to rectifies is supplied by 0.5÷3 kV/ 1 kA/ 2 kHz invertors.

2.2. Negative ion beam production and transport study

The experiments on negative ion beam formation, acceleration and transport through the LEBT and HEBT were carried out for the 0.65 A, 85 keV primary beam with pulse duration of 2.5 s.

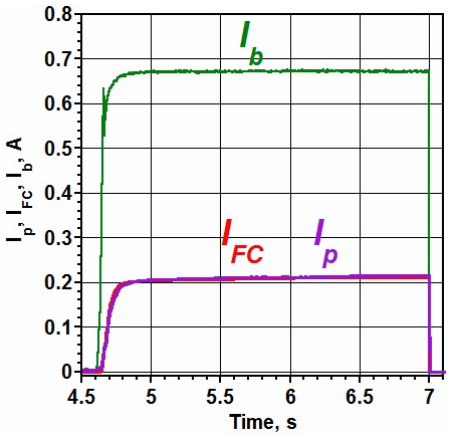

FIG. 4. Typical oscillograms of the outgoing H^- current I_b, of FC current and of acceleration tube current I_p

Fig. 4 shows the typical oscillograms of H^- beam currents registered. I_b is a current, measured as a difference of the total current in the accelerated circuit and of current, intercepted to the acceleration grid [7]. I_{FC} is a H^- beam current, measured by ø17 cm Faraday cup (FC) located in the LEBT tank at the distance 2.5 m away from the source. I_p is a current in the acceleration tube circuit (see Fig.2). The differential current I_b consists mostly of H^-

ions outgoing from the source [3]. As it is shown in Fig. 4, in the case of outgoing current I_b of about 0.68 A the acceleration tube current I_P is about 200÷230 mA. It corresponds to the recorded beam transmission of 30÷34%. The typical distribution of the beam current density, obtained by scanning with the movable ø10 mm FC is shown in Fig. 5. The black dots of profile in Fig. 5 show the positions, at which the current was measured. The 2D profile of the beam current density was obtained by the interpolation of the density calculated at the points of measurements. The individual beamlets produced at the exit of ion source are mixed at the distance 2.5 m due to beamlet divergence. The total beam current integrated over FC plane is $\oint\oint jdS$ = 415 mA. The red circle shows the position and shape of ø170 mm FC, when the current was registered. The calculated value of FC current is 200 mA, which matches with the measured value. The fraction of FC current equals to 48% of the total beam current at FC plane, and the blue circle shows the area, which covers 80% of the total beam current. Assuming the initial beam size of 124 mm, we can estimate the beam angular divergence as $\alpha = \pm 25\ mrad$. Obtained divergence value is in a good agreement with IBSIMU calculations described in [4]. The integrated beam current at FC plane is equal to 71% of the beam current measured at the source exit due to the beam stripping in the vicinity of the ion-optic system and during transport though the LEBT tank [5]. Left satellite in the current density profile, which can be seen in Fig. 5, is produced by leftmost baemlets deflected in the source ion-optical system due to aberrations caused by the slit geometry of the acceleration electrode [4].

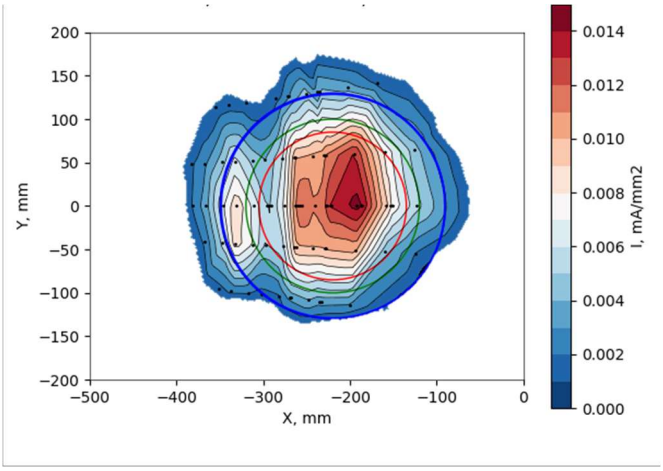

FIG. 5. Profile of beam current, measured by movable FC at the distance of 2.5 m. The dots show the positions, at which the current was measured by ø10 mm FC. RF driver with Faraday screen. RF power 30 kW, extraction and acceleration U_{ex}+U_{ac} = 6.5 + 77.5 keV, hydrogen filling pressure P_{H2} = 0.4 Pa; I_b = 0.58 A, I_{HV} = 0.19 A.

The dependencies of the source exit current I_b and of the acceleration tube current I_p versus extracted voltage U_{ex} are shown in Fig. 6.

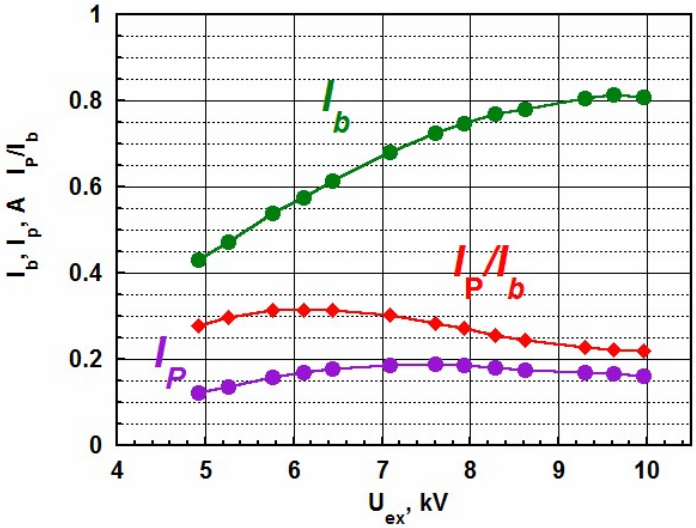

FIG. 6. Dependencies of source exit current I_b (green) and of accelerated current I_p (purple) vs extraction voltage U_{ex}. The ratio I_p / I_b is plotted in red. Empty circles –hydrogen filling pressure P_{H2}= 0.5 Pa, RF discharge power P_{RF}= 30 kW; filled circles –P_{H2}=0.42 Pa, P_{RF}=28 kW. The initial beam energy 84 keV, acceleration tube voltage 158 kV.

An increase of extraction voltage in the range of U_{ex}= 4÷7 kV produces the beam current I_b growth from 0.4 to 0.7 A, while the acceleration tube current I_p increases up to 0.18÷0.2 A and is maximal at U_{ex}≈ 7 kV. The variation of the extraction voltage changes the emission plasma meniscus shape and influences the beamlet angular divergence. The I_p/I_b ratio of Fig. 6 reflects the beam transmission and it depends on initial beam energy and on H^- beam divergence. The maximum value of I_p/I_b = 33% was achieved at U_{ex}= 6.5 kV, which corresponds to the optimal plasma meniscus shape at the given emission current density. The extraction voltage should be varied in accordance with the acceleration voltage to prevent an additional beam defocusing in the source acceleration gap. The maximal IOS voltages were limited by power supplies and have the value of $U_b = U_{ex} + U_{ac} < 85$ kV.

2.3. Beam transport efficiency

The parameters of beam formation, of beam transport efficiency and acceleration obtained in various cases are summarized in the Table 1. The column U_{ex} in the table shows the value of the source extraction voltage, columns U_b and I_b show NI beam energy and current at the source exit. Next 3 columns show beam transport efficiency to different z-axis positions: to distances 2.5 m, 3.8 m, and 4.45 m. At z = 2.5 m the fraction of the current registered by FC I_{FC}/I_b is shown. At the other two positions there are limiting apertures with different sizes indicated in brackets. At z = 4.45 m the ratio of the current entering acceleration tube after aperture ø200 mm to the ion source current I_p/I_b is shown. The transport efficiency measurements for experimental cases #3 and #4 were done earlier [5]. The transport efficiency after square aperture 240x240 mm located at z = 3.8 m was measured in this case. The beam acceleration for cases #3 and #4 have not been conducted.

TABLE 1. BEAM PRODUCTION AND TRANSPORT EFFICIENCY

	U_{ex}	U_b	I_b	z=2.5 m (ø170 mm)	z=3.8 m (240x240 mm^2)	z=4.45 m (ø200 mm)
Case #1	6.5 kV	84 kV	0.65 A	31%	-	32%
Case #2	10 kV	85 kV	0.77 A	25%	–	21%
Case #3	7 kV	82 kV	0.6 A	-	50%	-
Case #4	10 kV	93 kV	0.9 A	–	60%	–

All cases #1÷4 shown in Tab. 1 were made at the similar RF driver operation parameters. In the case #1 the extraction voltage of 6.5 kV for the beam with current 0.65 A provides optimal beam transport efficiency. About 31% of the beam was measured by FC at 2.5 m with total 32% transmission to the entrance of acceleration tune after diaphragm ø200 mm at 4.45 m. In the case #2 the source extraction voltage was increased to 10 kV at the fixed total beam energy 85 kV. In this case, the fraction FC registered current at 2.5 m decreases from 31% to 25%, and the beam transport efficiency to the distance of 4.45 m from 32% to 21%, which corresponds to increased beam divergence. The case #3 demonstrates the transport efficiency measurements to 3.8 m distance for the beam current, extraction voltage, and total energy similar to the case #1 with optimized beam angular divergence for total energy 84 keV. The measurements for experimental case #4 was done at the higher total beam energy of 93 keV and higher extraction voltage 10 kV. It shows higher beam transport efficiency 60% compared to 50% for the 84 keV case.

According to the results of computer modelling using COMSOL software the beam transport efficiency with beamlet divergence of 30 milliradians at z = 3.8 m after 240x240mm^2 aperture is 82 %, and after the diaphragm ø200 mm located at z = 4.45 m is 55%. These values did not include the beam stripping. To estimate beam stripping we can use measured earlier values for the beam stripping at the source output 15% [5] and during the beam transport at the residual hydrogen pressure of $3\cdot10^{-3}$ Pa during the operation pulse 3%/m [5]. The efficiency of the beam transport, taking into account the stripping, are 60% for z = 3.8 m and 39% for z = 4.45 m. The beam transport efficiency in case #4 is in a good accordance with COMSOL 30 mrad simulation.

3. FULL-SCALE NEGATIVE ION SOURCE PROJECT

The full-scale RF H^- source with the projected total negative ion beam current 9 A, energy up to 120 keV and pulse duration up to 100 s was designed at BINP. The cross-section view of the source is shown in Fig. 7. It includes four RF plasma drivers, attached to the Ø700 mm expansion plasma chamber, and the 4-electrodes IOS, forming the beam with 142 beamlets. The emission current density of single beamlet is 25 mA/cm^2. An additional pumping of the IOS area through the peripheral windows in the IOS chamber is projected. IOS electrodes thermo stabilization by circulating of thermal carrier through the internal channels will be provided.

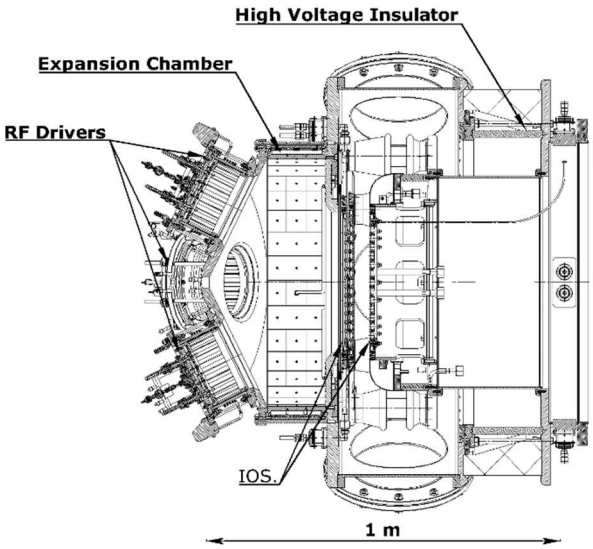

FIG. 7. The cross-section view of the projected full-scale negative ion source.

4. PROTOTYPE OF PLASMA NEUTRALIZER

The prototype of plasma neutralizer was constructed, and it experimental study was performed at the separate test bench. The photo of neutralizer is shown in Fig. 9. The complex magnetic field configuration of the neutralizer is produced by an array of circular permanent magnets. This configuration (multicusp at the walls, longitudinal in the plasma volume with the inversed end mirrors) provides the plasma confinement. Plasma is generated by the arc discharge with LaB_6 cathodes, installed at the periphery of the central plane. Working gas (hydrogen) is injected to the chamber center. It was observed, that the considerable negative potential develops in the plasma, decreasing the ion outflow, and the plasma losses through the ends are suppressed by the inverse magnetic mirrors. It was founded that a relatively low power of the discharge is required to sustain $\sim 10^{19}$ m^{-3} density plasma in the plasma neutralizer prototype with the inverse end mirrors [6].

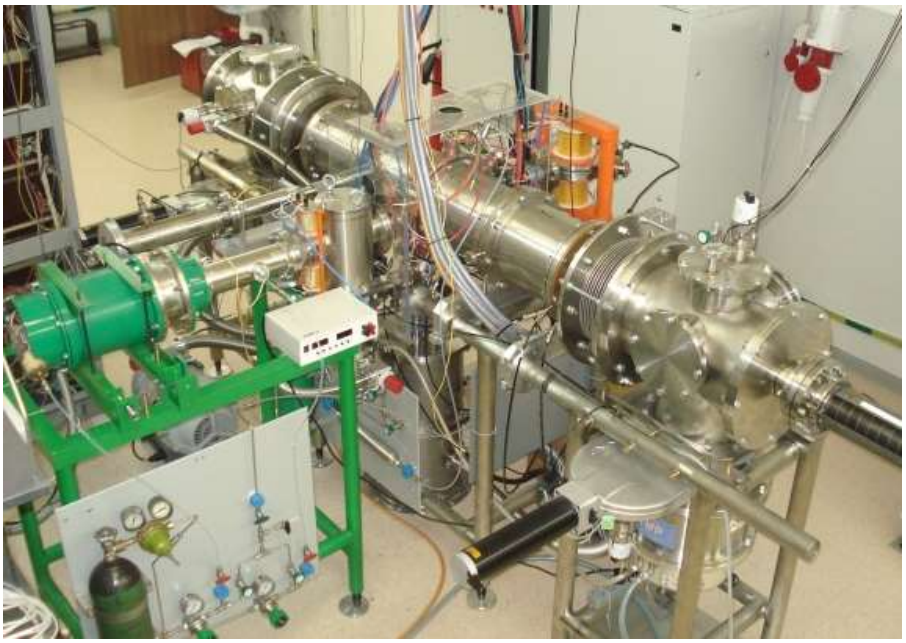

FIG. 8. H^- beam neutralization test bench with plasma neutralizer prototype.

5. SUMMARY

The first experiments on negative ion beam acceleration and transport through the LEBT and HEBT were carried out at the BINP high voltage injector prototype. The beam was post-accelerated from initial energy 84 keV to

energy 242 keV, and up to 35% of the produced 0.6 A H^- beam was transported to the calorimeter in these experiments. The beam compression by wide-aperture quadrupole magnets was successfully tested. The obtained data on beam angular divergence and transport efficiency is in a good agreement with the COMSOL and IBSIMU calculations. The transport efficiency can be increased up to 90% due to increase of the beam initial energy up to projected 120 keV, and enlarging of the acceleration tube inlet aperture diameter from 20 to 26 cm.

The full-scale RF H^- source with the negative ion beam current 9 A at the energy of 120 keV and the pulse duration up to 100 s was designed and now is under manufacturing and assembling.

The prototype of plasma neutralizer was constructed and tested. It was founded that a relatively low power of the discharge is required to sustain plasma density $\sim 10^{19}$ m^{-3} in neutralizer with the inverse end mirrors.

REFERENCES

[1] A.A. Ivanov, G.F. Abdrashitov, V.V. Anashin et al., Development of a negative ion-based neutral beam injector in Novosibirsk, AIP Conf. Proc. **1515**, 197 (2013)

[2] H.P.L de Esch and M. Singh, Electron dumps for ITER HNB and DNB beamlines, Fusion Eng. Des. **85**, 707 (2010)

[3] Yu. Belchenko, G. Abdrashitov, P. Deichuli, AA. Ivanov, A. Gorbovsky, A. Kondakov, A. Sanin, O. Sotnikov and I. Shikhovtsev, Inductively driven surface-plasma negative ion source for N-NBI use (invited), Rev. Sci. Instrum., **87**, 02B316 (2016)

[4] O. Sotnikov, A. Sanin, Yu. Belchenko, A. A. Ivanov, G. Abdrashitov, A. Belavsky, A. Gorbovsky, A. Donin, P. Deichuli, A. Dranichnikov, A. Kondakov, I. Shikhovtsev., Negative ion beam acceleration and transport in the High voltage injector prototype, to be published at AIP Conf. Proc. (2021)

[5] Yu. Belchenko, A.A. Ivanov, A. Sanin, O. Sotnikov, AIP Conf. Proc., Extracted beam and electrode currents in the inductively driven surface-plasma negative hydrogen ion source, **1869**(1), 030005 (2021)

[6] S. Emelev and A. Ivanov, A plasma target for neutralization of the negative ion beam, AIP Conf. Proc. **2052**, 070005 (2018)